All the Covers of the Horseshoe

Robert Gilmore†, Arunasri Nishtala †, and Tsvetelin D. Tsankov‡

† Physics Department, Drexel University, Philadelphia, Pennsylvania 19104, USA
‡ Physics Department, Bryn Mawr College, Bryn Mawr, PA 19010, USA

E-mail: robert.gilmore@drexel.edu

Submitted to: *Nonlinearity*

Abstract. The Lorenz attractor can be mapped to a Rössler-like strange attractor by a local $2 \to 1$ mapping. Conversely, the Rössler attractor can be lifted to a Lorenz-like attractor by the inverse map. It can also be lifted to many other inequivalent covering strange attractors. We classify all possible lifts of Rössler-like strange attractors exploiting an analogy between dynamical systems theory and Lie group theory.

PACS number: 05.45.Ac

1. Introduction

The properties of a strange attractor are unchanged under a nonsingular change of variables ("global diffeomorphism"). These mappings simply produce a deformation of the attractor. Local diffeomorphisms do produce changes in the properties of strange attractors. For example, the $2 \rightarrow 1$ local diffeomorphism $u = x^2 - y^2, v = 2xy, w = z$ maps the Lorenz attractor (variables (x, y, z)) into a strange attractor that is topologically similar to the Rössler attractor (variables (u, v, w)). Running the local diffeomorphism the "other way" ($(u, v, w) \rightarrow (x, y, z)$) generates a $1 \rightarrow 2$ covering attractor from an image attractor. Local diffeomorphisms act on dynamical systems in much the same way that local isomorphisms relate the Lie groups $SU(2)$ and $SO(3)$ to each other as covering and image Lie groups.

It has been pointed out that three subjects that play an important role in physics share many similarities. These subjects are Lie group theory [1], singularity (or catastrophe) theory [2], and dynamical systems theory [3]. As a consequence, results valid for any of these theories could have important analogs in the others. The role of local isomorphisms in Lie group theory is expressed in a very beautiful theorem due to E. Cartan [1]. It has been suggested that this theorem ought to have an analog in dynamical systems theory [3]. The purpose of the present work is to state what this result is and to provide examples of its application. This is done for "low-dimensional" strange attractors: those with Lyapunov dimension $d_L < 3$ that can be described by knot-holders [3, 4, 5, 6].

In Sec. II we review Cartan's theorem: how it relates a Lie algebra to a unique universal covering Lie group, and how all other Lie groups with the same Lie algebra are obtained from the covering group by local isomorphisms. In Sec. III we review what is known about image and covering dynamical systems that are related by local diffeomorphisms. These results are provided concrete form in terms of simple examples, given in Sec. IV. In Sec. V we describe all possible lifts of a particular image dynamical system. This is the system which is seen most frequently in the topological analysis of experimental data. This system generates chaos and strange attractors through the Smale horseshoe stretch and fold mechanism. The mechanism is represented by a knot-holder, or branched manifold. All its lifts are represented by covering knot-holders. In Sec. VI we describe the spectrum of orbits in the covering dynamical system that map to a particular orbit in the image dynamical system. We also describe how to lift nonperiodic (chaotic) orbits into covers. In Sec. VII we introduce indices for image and covering orbits. The index of an image orbit is a permutation group operation, and can be described by a set of cycles. It has a multiplicity of interpretations. The covering orbits satisfy several topological index results. We describe how to compute linking numbers of lifted periodic orbits in Sec. VIII. In Sec. IX we describe the most general lift of the image branched manifold into covering branched manifolds. In the final Section we identify the structures in a Lie group (image and cover) with the structures in a dynamical system (image and cover) that make this analogy work so well.

2. Lie Groups and Local Isomorphisms

The study of Lie groups is simplified by linearizing the group in the neighborhood of any of its group operations: in particular the identity. The group structure in this linearization is preserved in the group's Lie algebra. In particular, the group properties are preserved in the structure constants of the Lie algebra [1].

A Lie group can be recovered from a Lie algebra by the exponential mapping. However, there is not a 1:1 correspondence between Lie groups and Lie algebras. Different Lie groups can have the same Lie algebra: the best known example is the Lie group pair $SO(3)$ and $SU(2)$, which have isomorphic Lie algebras — the angular momentum algebra. Lie groups with the same Lie algebra are *locally* isomorphic but may not be *globally* isomorphic.

Cartan has provided a beautiful theorem relating Lie groups and their algebras. The theorem states that there is a 1:1 correspondence between a Lie algebra and a particular Lie group. This Lie group is simply connected — this is a topological property. All other Lie groups with the same Lie algebra are constructed algorithmically from this simply connected group. The construction proceeds by dividing (taking the quotient of) the simply connected group by one of its discrete invariant subgroups. For this reason the simply connected group is called the *universal covering group*, since in some sense it covers all Lie groups with the same Lie algebra. The original simply connected group and its quotients are *locally* isomorphic but not *globally* isomorphic.

Cartan's theorem identifies all the operations in the covering group $\overline{G}$ ($SU(2)$) that map to the identity group operation in some non-simply connected Lie group G ($SO(3)$) with the same Lie algebra. The standard way to identify different group operations (e.g., $+I_2$ and $-I_2$ in $SU(2)$) in a subgroup D is to "mod them out," that is, to divide by them. Division of a group by a subgroup $\overline{G}/D$ creates a group G only when the subgroup D is invariant in $\overline{G}$. Further, division reduces the dimension of $\overline{G}$ by that of the subgroup D. Since the Lie groups $\overline{G}$ and G must have the same dimension (their Lie algebras are isomorphic), the subgroup D is not continuous. That is, it is a discrete invariant subgroup of $\overline{G}$.

3. Dynamical Systems and Local Diffeomorphisms

Two dynamical systems are equivalent if they are *globally* diffeomorphic. This means that there is some differentiable coordinate transformation that maps one continuously into the other. Diffeomorphic dynamical systems, and their strange attractors, are not topologically distinguishable [3].

It is possible for two dynamical systems to be locally diffeomorphic everywhere but not globally diffeomorphic. In this case they are not equivalent [7, 8, 9]. In general it is possible to distinguish locally diffeomorphic dissipative dynamical systems by the global connectivity properties of their attractors [10, 11]. In this way dynamical systems theory and Lie group theory exhibit striking parallels.

The question has been raised if there is some theorem that does for dynamical systems what Cartan's theorem does for Lie algebras and their Lie groups, including the universal covering group [3]. For Lie groups there is a "largest" group (the universal covering group) and all others with the same Lie algebra are locally isomorphic $n \to 1$ images.

We investigate the possibility of a similar correspondence in the case of dynamical systems. In this work we consider the class of dissipative dynamical systems that possess strange attractors with Lyapunov dimension $d_L < 3$. For such dynamical systems there is some "smallest" attractor: all others that are locally diffeomorphic are $1 \to n$ lifts, or covers. So the question for attractors of dynamical systems that corresponds to Cartan's theorem for Lie groups is: How many covers does an image attractor possess, and how can these covers be characterized?

We treat this question here in the context of an image attractor described by a knot holder, or branched manifold, that describes the Smale horseshoe ("stretch and fold") mechanism [3, 4, 5, 6]. The objective of this work is to list all possible covers of this dynamical system. These covers will be described by their branched manifolds. All the covers of other image attractors can be constructed following the prescription given here for the Smale horseshoe strange attractor.

4. An Example

Locally diffeomorphic systems have been studied in detail by Miranda and Stone [7] and by Letellier and Gilmore [8, 9]. Typically a local diffeomorphism creates a $2 \to 1$, or more generally an $n \to 1$, relation between a covering attractor and its image attractor. For example, the local diffeomorphism $u = x^2 - y^2,\ v = 2xy,\ w = z$ is a $2 \to 1$ map of the Lorenz attractor to an image attractor that is topologically equivalent to the Rössler attractor. Conversely, the Rössler attractor can be "lifted" to a double cover (similar to $SO(3) \uparrow SU(2)$) using the inverse mapping.

An attractor can be lifted to a locally diffeomorphic cover in a number of different ways. Figure 1(a) shows the right-handed Smale horseshoe branched manifold and figure 1(b) shows two different lifts of it. One of these covers has rotation symmetry, the other has inversion symmetry [8]. The two differ in the direction of rotation of the branch connecting the branch line on the right with the branch line on the left: one has a right-handed twist (top), the other a left-handed twist (or "helicity").

The return map of the branch line B back to itself for the Smale horseshoe branched manifold is shown in figure 2(a). It is a simple unimodal map of the interval. The return map for either of the double covers of figure 1(b) is shown in Figure 2(b) [12]. The two branched manifolds in figure 1(b) each have two branch lines, labeled L and R. Initial conditions on L can map either back to L, if they are near the unstable focus in the hole near L, or map to R if they are further away along the branch line L. The map from L to L or from L to R occurs in one "topological period." Similarly, initial conditions along the branch line R map to R or to L during one topological period, depending on

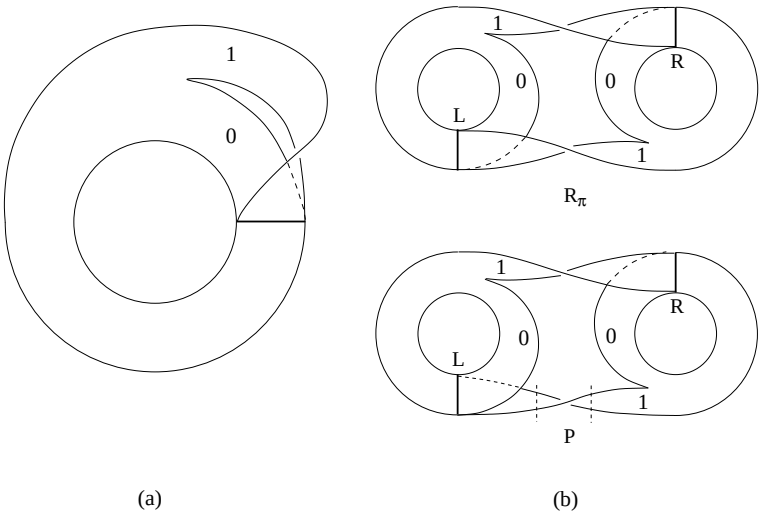

Figure 1. (a) Right-handed Smale horseshoe branched manifold. (b) Two covers of the horseshoe branched manifold, one with rotation symmetry, one with inversion symmetry. Both are locally diffeomorphic with the Smale horseshoe branched manifold.

how close they are to the unstable focus near R. In the return map for these double covers, we adopt the convention that the branch lines are measured from the inside (near the focus) to the outside of the attractor, from left to right. Such a convention is always applicable to the covers treated below [11].

The branches of the return maps for the double covers are labeled by symbols 0 and 1. Under the $2 \to 1$ local diffeomorphism, the two parts of the return map labeled 0 map to the single branch labeled 0 of the Smale horseshoe return map, and similarly for the parts of the return map labeled 1. In order to distinguish the two double covers, their return maps must be "dressed" by additional information. This includes local torsion information as well as information about the order in which the branches are joined at the branch line [3, 6]. For example, for the double cover with $R(\pi)$ symmetry (figure 1(b), top) the local torsions are 0 on the branches labeled 0 and $+1$ on the branches labeled 1. For the double cover invariant under P (inversion), the branch labeled 1 over R has local torsion -1 [8]. Local torsion is measured in units of π. Local torsion ± 1 is a half twist.

The two double covers of the Smale horseshoe branched manifold (figure 1(b)) are composed of two types of units. These are illustrated in figure 3. One unit (figure 3(a)) describes the squeezing and stretching mechanisms that act to build up strange attractors. This unit includes one branch line, B. Flowing into B are two branches from different parts of the attractor — or the branched manifold that represents the attractor. Flowing out of B are two branches that carry the flow off to two different parts of the attractor. The inflow to B describes squeezing, the outflow from B describes stretching. The other components of the double covers, and all other covers that we describe below, are simple "flow tubes" or branches, illustrated in figure 3(b) and (c). Flow tubes carry the outflow from a unit of the type shown in figure 3(a) to the input of

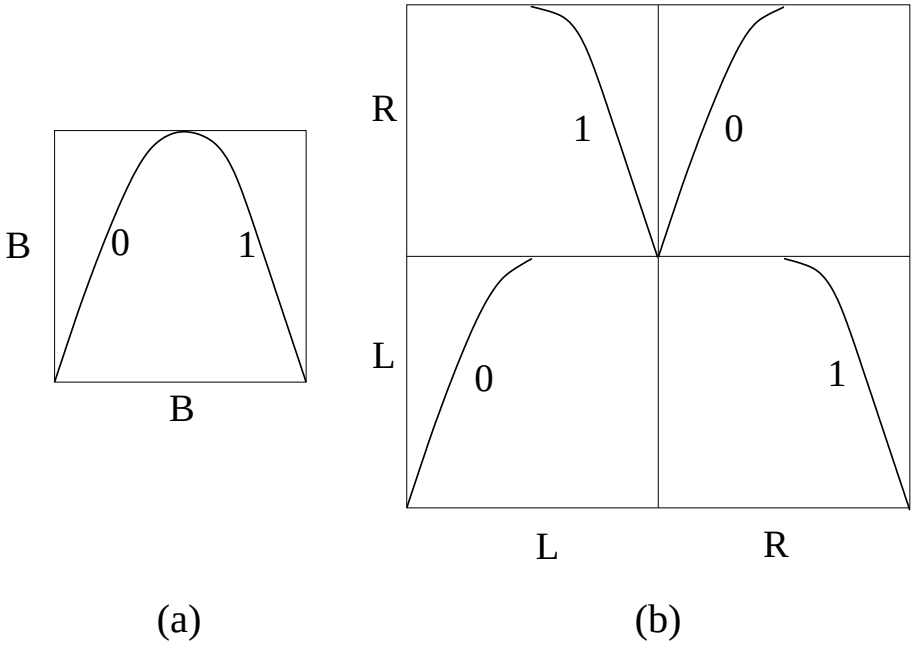

Figure 2. (a) Return map of the Smale horseshoe branched manifold. (b) Return map for the two double covers shown in Figure 1. The two branched manifolds are distinguished by dressing the branches 0, 1 over L and R with local torsion information.

another (possibly the same) unit of this type. One flow tube is shown between the two vertical dashed lines at the bottom of figure 1(b). The flow tubes shown in figure 3(b) are orientation-preserving and have even local torsion $(0, \pm 2, \pm 4, \ldots)$. Those shown in figure 3(c) have are orientation-reversing and have odd local torsion $(\pm 1, \pm 3, \ldots)$. In lifts of the horseshoe branched manifold in figure 1(a), branches that cover the orientation-preserving branch of the horseshoe labeled 0 must have even local torsion. Flow tubes that cover the orientation-reversing branch of the horseshoe labeled 1 must have odd local torsion.

5. General Lifts

A locally diffeomorphic lift (cover) of the horseshoe strange attractor can be represented by its knot-holder (branched manifold). The knot-holder for an n-fold cover is composed of n units of the type shown in figure 3(a) [3, 4, 5, 6, 8, 12]. These are connected to each other by $2n$ flow tubes. For tearing [12] that occurs at the maximum of the return map (cf. figure 2(b)) n branches are orientation-preserving, of the type shown in figure 3(b), and n are orientation-reversing, of the type shown in figure 3(c). In this work we will consider only connected covers, where each branch line is accessible from every other branch line.

Every strange attractor in R^3 can be classified by a branched manifold. A remarkable recent result guarantees that branched manifolds can themselves be classified by topological surfaces called bounding tori [10, 11]. These are two-dimensional closed

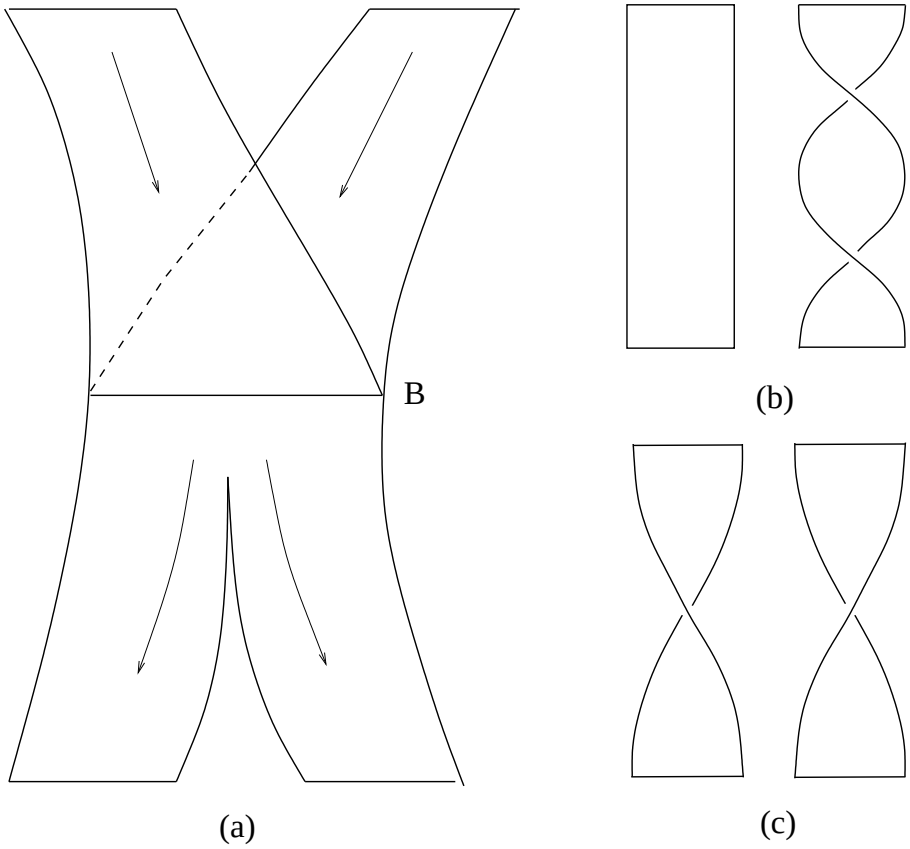

Figure 3. (a) In locally diffeomorphic lifts all building blocks containing a branch line are equivalent. The parts of the branched manifolds between two branch lines can have (b) zero local torsion or local torsion different by integer multiples of 2π ($L \to L$ or $R \to R$); or (c) odd local torsion ($L \to R$ or $R \to L$).

surfaces with non-zero genus that are dressed with a flow. The flow is obtained after "inflating" the semi-flow on the branched manifold back to a three-dimensional flow defined inside a two-dimensional surface that encloses the branched manifold. The inflation is done so that the three-dimensional flow has the same limiting properties as the semi-flow on the branched manifold. The surface flow is defined on a closed two-dimensional surface (with non-zero genus) and so it is structurally stable [13]. The fixed points for this boundary surface flow will be saddles due to the fact that the Lyapunov dimension of the considered strange attractors is $d_L < 3$. Thus in a plane transverse to the chaotic flow, upon linearization we obtain one stable and one unstable direction. These bounding tori together with their associated surface flow can be conveniently represented in terms of canonical forms [11].

One such canonical form is shown in figure 4. This is one of two canonical forms that can arise in experiments that generate data with one more level of complexity than the Lorenz attractor [14]. In that case the time series $x(t)$ oscillates around two unstable foci. When a dynamical system generates data $x(t)$ that oscillate around three unstable foci (A, B, C), the time trace can enter the neighborhood of these fixed points cyclically,

$A \to B \to C \to A$ etc., or can oscillate $A \leftrightarrow B \leftrightarrow C$. These two behaviors are described by two canonical forms, and are the only behaviors that can occur with three unstable foci.

The canonical form shown in figure 4 is a projection of a torus of genus five (there are five holes) onto a plane. This canonical form is useful for describing the case of three unstable foci exhibiting dynamics $A \leftrightarrow B \leftrightarrow C$. Under this projection we obtain a planar surface - a punctured two-disk with the same genus as the genus of the original bounding surface. All the singularities in the boundary surface flow occur around two of the holes (four singularities per hole). The two holes in figure 4 that have singularities are shown as squares, dressed appropriately with one-dimensional flow (pictured as arrows). The remaining three holes are shown round: they correspond to unstable foci of the actual chaotic flow. In general, the structure of the canonical form is determined by the fact that the coexisting unstable fixed points determine the large scale structure of a strange attractor. In that context the two squares correspond to regular saddles of the three-dimensional flow.

The exterior boundary of the canonical form is provided with an orientation [10, 11]. In this projection the orientation is clockwise and it describes the direction of the semi-flow on any enclosed branched manifold. The round holes are labeled with one type of symbol (A, B, C) and the holes with singularities are labeled with a different type of symbol (a, b). The order in which these holes are encountered in a round trip around the exterior boundary uniquely labels the canonical form [10, 11] (up to cyclic permutation). For the genus-5 canonical form shown, the label can be chosen as the four-symbol string $ABCB$ or dually as the four-symbol string $abba$. A strange attractor that can be enclosed in a genus-g torus has a Poincaré section that consists of $g - 1$ disjoint disks. The four disks are represented as short line segments labeled 1 through 4 in figure 4. They are numbered in the order in which they are encountered in a round trip along the exterior boundary. For any branched manifold contained in the corresponding genus-5 bounding torus, all branch lines can be moved to one of the four components of the Poincaré section. The transition from one component to an adjacent component (in the sense of the flow) is called a topological period.

The connectivity properties of a branched manifold enclosed by a bounding torus are described by a transition matrix. The transition matrix describes the two components of the global Poincaré surface of section that can be reached in one topological period from each of the components. That is, $T_{ij} = 1$ if an initial condition on component i can reach component j in one topological period. Since initial conditions on each component flow to exactly two other components, the transition matrix can be written as the sum of two permutation matrices $T = T_{\rm str} + T_{\rm cyc}$. The two matrices for the canonical form shown in figure 4 are

$$T_{\rm str} = \begin{bmatrix} 1 & 0 & 0 & 0 \\ 0 & 0 & 0 & 1 \\ 0 & 0 & 1 & 0 \\ 0 & 1 & 0 & 0 \end{bmatrix} \qquad T_{\rm cyc} = \begin{bmatrix} 0 & 1 & 0 & 0 \\ 0 & 0 & 1 & 0 \\ 0 & 0 & 0 & 1 \\ 1 & 0 & 0 & 0 \end{bmatrix} \tag{1}$$

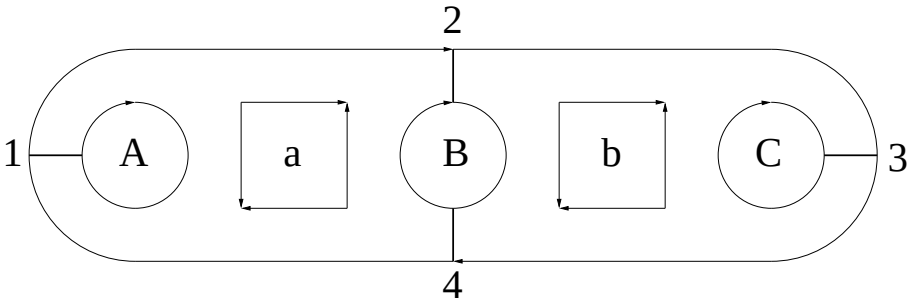

Figure 4. A canonical form with genus 5. The global Poincaré surface of section has $4 = g - 1$ components, each connected to a round hole free of singularities (A, B, C). These summarize motion around unstable foci. The two "square" holes (a, b) have four singularities each, and describe motion in the neighborhood of regular saddles.

The cyclic matrix $T_{\rm cyc}$ describes the flow around the exterior boundary. The other matrix, $T_{\rm str}$, defines the structure of the bounding torus [10, 11, 15].

A $1 \to 4$ cover of the horseshoe branched manifold is contained in a bounding torus whose genus g is determined from $4 = g - 1$. In figure 5 we show one possible four-fold cover of the horseshoe branched manifold that is contained in the bounding torus of figure 4. This is one possible double cover of the Lorenz attractor, or four-fold cover of the Rössler attractor, without any symmetry. The 4-fold cover of the horseshoe has four branch lines, each of which covers the (one) branch line in the image. Each branch line can be placed in one of the components of the global Poincaré surface of section. In fact, each branch line in the cover is part of a squeeze-and-stretch unit (figure 3(a)). These units are all identical (locally homeomorphic) with each other and with the corresponding unit in the image.

This particular lift has one (and therefore all) exterior branches covering the orientation-reversing branch 1 of the horseshoe branched manifold. We have chosen the torsion of each of these branches to be $+1$, except for the branch joining branch line 2 to branch line 3, with torsion -1. This branched manifold corresponds to a covering strange attractor which cannot be obtained from the image attractor by applying a local diffeomorphism that obeys a discrete symmetry [8, 9]. The structure of the covering branched manifold can be specified by a matrix Tor, obtained by dressing the transition matrix T [equation (1)] with helicity information:

$$T = \begin{bmatrix} 1 & 1 & 0 & 0 \\ 0 & 0 & 1 & 1 \\ 0 & 0 & 1 & 1 \\ 1 & 1 & 0 & 0 \end{bmatrix} \quad \longrightarrow \quad Tor = \begin{bmatrix} 0 & +1 & * & * \\ * & * & -1 & 0 \\ * & * & 0 & +1 \\ +1 & 0 & * & * \end{bmatrix} \begin{matrix} 1 \\ 2 \\ 3 \\ 4 \end{matrix} \tag{2}$$

In this matrix the nonzero matrix elements of the transition matrix $T = T_{\rm str} + T_{\rm cyc}$ are replaced by integers that specify the local torsion of the branch connecting branch line i to branch line j. For example, the branch carrying the flow from branch line 2 to branch line 3 is left handed with helicity -1, so that $(Tor)_{23} = -1$.

The return map on this branched manifold is presented in figure 6. This return map shows that initial conditions along the outer half of each branch line (i) flow to the next branch line ($i+1$). Initial conditions on the inner half, closer to the unstable focus inside each round hole, flow to a branch line determined by $T_{\rm str}$. For example, $f(i)$ is defined from figure 4 and $T_{\rm str}$ to be

i	1	2	3	4
$f(i)$	1	4	3	2

The return map must be further dressed by helicity information over each branch i.

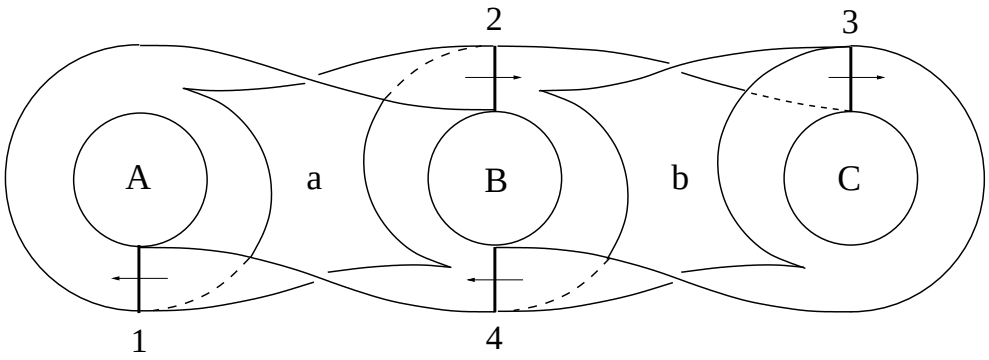

Figure 5. One four-fold cover of the horseshoe branched manifold that can be enclosed by the bounding torus shown in figure 4.

6. Lifts of Orbits

Every orbit in the image attractor lifts to one or more orbits in the covering attractor. This is true for periodic orbits as well as non-periodic (chaotic) orbits. The symbol sequence for a lift depends on the symbolic name of the image orbit and the initial condition in the cover. We consider in the following two subsections lifts of periodic orbits and non-periodic (chaotic) orbits.

6.1. Periodic Orbits

For local diffeomorphisms generated by a discrete group G, an orbit of period p in the image lifts to $|c|$ orbits of period $|h| \times p$ in the cover, where $|c| \times |h| = |G|$ and $|G|$ is the order of (number of group operations in) G. The $|c|$ orbits are mapped into each other by the group operations in G [8, 9].

A richer spectrum of possibilities exists for $n \to 1$ local diffeomorphisms. In this case an image orbit of period p lifts to one or more orbits. The lifts generally have different periods. The total number of symbols in all the covering orbits is $n \times p$, and each symbol $1, 2, \ldots, n$ occurs exactly p times. The distinct lifts are described by an index. The index is an operation in the permutation group S_n $n = g - 1$. Every permutation group operation can be expressed as a product of cycles.

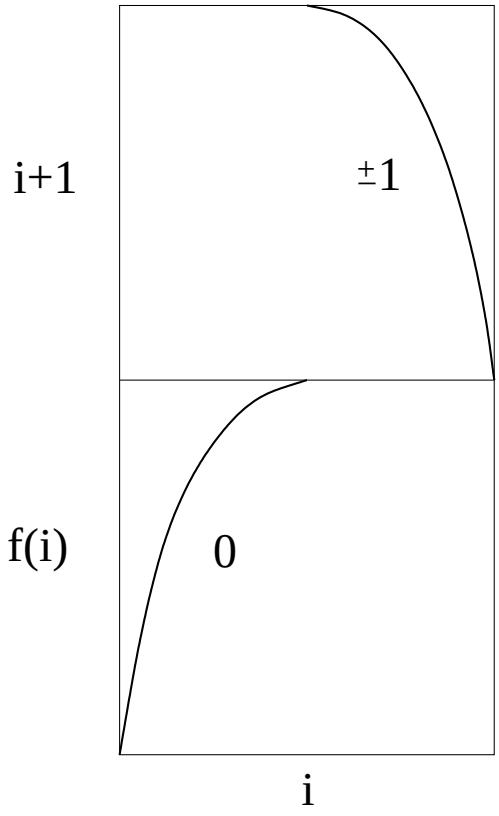

Figure 6. Return map for a cover of the Smale horseshoe branched manifold contained in a bounding torus of any genus g, $g \geq 3$. The numbering of the branch lines is canonical, and the function defined by $i \to f(i)$ is determined from the permutation matrix $T_{\rm str}$.

These statements will be illustrated by lifting the period-3 orbit 011 in the image attractor (its branched manifold) into the four-fold cover shown in figure 5 ($p = 3, n = 4, g = 5$). The period three orbit in the image is shown in figure 7. The three intersections of this orbit with the branch line B are labeled α, β, γ, in the order of occurrence. Under the local diffeomorphism, four units of the type shown in figure 3(a) are identical to each other and to the single unit of this type in the image attractor. As a result, all four branch lines in the four-fold cover exhibit intersections α, β, γ that are identical to those in the image branched manifold.

A lift of 011 with initial conditions on branch line 1 at α will propagate, in one period, back to point β on branch line 1. During the next topological period the transition $\beta \to \gamma$ will occur (over the image). Further, the flow will propagate to branch line 2. During the third topological period $\gamma \to \alpha$ and $2 \to 3$. Proceeding further, after six topological periods we find $(1\alpha \to 1\beta \to 2\gamma \to 3\alpha \to 3\beta \to 4\gamma \to 1\alpha)$. Thus we obtain a lift of 011 with topological period 6 and symbolic name 112334. The situation is illustrated in figure 8. In a similar way we can lift the orbit 011 to different periodic orbits by starting at different initial conditions. For example starting at 1γ leads to a periodic lift 124 and starting at 2β we obtain 234. The sum of the periods is

$6 + 3 + 3 = 4 \times 3$ so that these are all possible lifts of the horseshoe period three orbit 011 using the four-fold cover branched manifold from figure 5.
The procedure for obtaining the periodic lifts can be represented in terms of the following permutation matrix

$$T_{(011)} = \begin{bmatrix} 0 & 0 & 1 & 0 \\ 0 & 1 & 0 & 0 \\ 1 & 0 & 0 & 0 \\ 0 & 0 & 0 & 1 \end{bmatrix} \begin{matrix} (1)123 \\ (2)412 \\ (3)341 \\ (4)234 \end{matrix} \tag{3}$$

The row labeled (1)123 tells us that an initial condition on branch line 1 (labeled (1)) over α in the image flows back to branch line 1 in the cover, since $T_{\rm str}$ tells us that $1 \to 1$. It also flows to the point β on this branch line, since α flows to β in the image. During the next topological period the flow in the lift over β in the image is from β on branch line 1 to γ on branch line 2 (according to $T_{\rm cyc}$), and during the third topological period $2\gamma \to 3\alpha$. Therefore the matrix element $(T_{(011)})_{13} = 1$ informs us that in the cover we visit (1)123, where (1) means that we start on branch line 1 over α. The other nonzero matrix elements in the permutation matrix $T_{(011)}$ are interpreted in the same way. The rows (and columns) of the matrix $T_{(011)}$ are labeled on the right by the sequence of components of the Poincaré section visited, starting from component (i). If initial conditions occur over β (or γ) we obtain the permutation matrix T_{110} (or T_{101}).

The permutation matrix T_{011} can be constructed simply by assigning a matrix to each symbol in the image orbit. In the present case the assignment is $0 \to T_{\rm str}$ and $1 \to T_{\rm cyc}$, so that $T_{011} = T_{\rm str}T_{\rm cyc}T_{\rm cyc}$. This assignment rule is true in general for lifts of all orbits from the image to every possible cover in any embedding torus. The reason for this assignment is that the lift of the orbits going through the orientation reversing branch of the horseshoe (1) is governed by the structure of the cyclic transition matrix $T_{\rm cyc}$ of the cover. Similarly the orbits going through the orientation preserving branch (0), when lifted to the cover, evolve under the structural transition matrix $T_{\rm str}$.

The product of the three matrices for the image orbit 011 is an operation in the permutation group, since it is the product of permutation matrices. This matrix is easily represented as a product of cycles in the standard fashion for permutation group operations: (13)(2)(4). This cyclic decomposition of the permutation matrix tells us that the period 3 orbit in the image lifts to three orbits of periods 2×3, 1×3, and 1×3 in the cover, since the component cycles have length 2, 1, and 1 and $p = 3$. The symbol sequence for these three orbits can be read from the row labels of the permutation matrix. For example, we decipher 13 as $(1\alpha)1\beta\ 2\gamma\ 3\alpha\ \ (3\alpha)3\beta\ 4\gamma\ 1\alpha$ or more simply as 123 341. The symbol sequences for all the lifts of 011 are

cycle	substitution sequence	symbol sequence
13	(1)123 (3)341	112 334
2	(2)412	124
4	(4)234	234

(4)

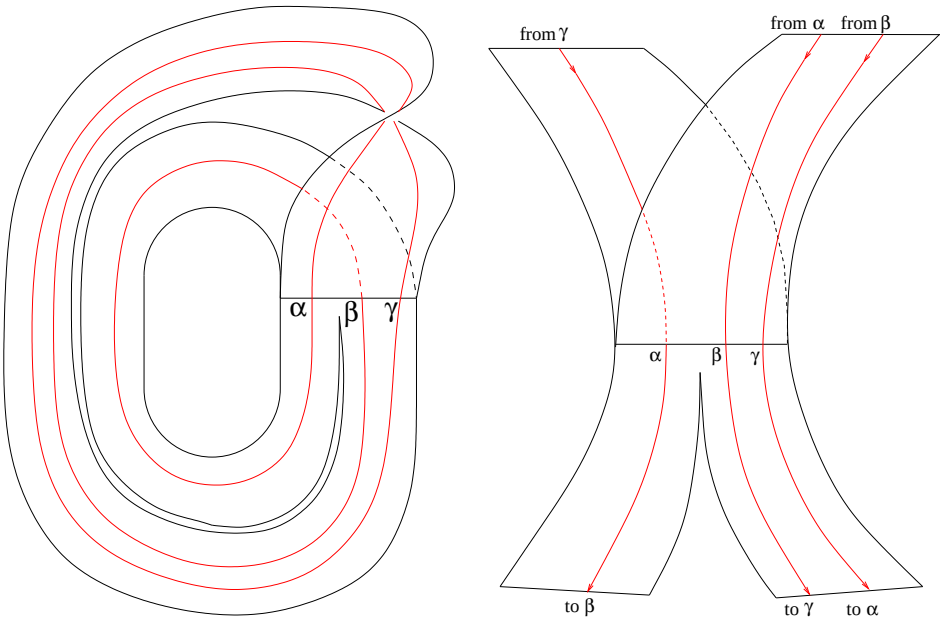

Figure 7. (a) Period three orbit 011 in the image attractor intersects branch line B in the order $\alpha \to \beta \to \gamma \to \alpha$, etc. (b) Each squeeze and stretch unit in the cover is locally diffeomorphic to the unit in the image, including the orbit segments that pass through each unit.

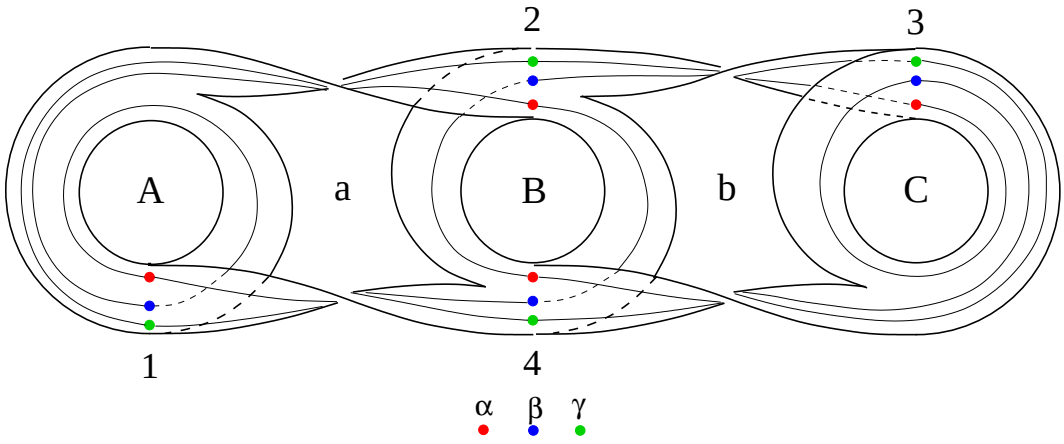

Figure 8. All three lifts of the horseshoe orbit 011 in the covering branched manifold of figure 5 are shown. By inspection the sum of the rotation indices for the lifts of 011 is $\sum(n_A, n_B, n_C, n_a, n_b) = (3, 3, 3, 2, 2)$.

Table 1. Orbits to period three in the image, a horseshoe branched manifold, are lifted into the covering strange attractor shown in figure 5. The cyclic structure of the permutation matrix and the full symbolic representation (symbolic dynamics) of the covering orbits are given.

Image Orbit	Cyclic Structure Permutation Matrix $T_{\rm orb}$	Symbol Representation Cover Orbit
0	1	1
	24	24
	3	3
1	1234	1234
01	12	11 24
	34	23 34
001	1234	112 423 334 241
011	13	112 334
	2	124
	4	234

The spectrum of the lifts of all orbits in the image is determined in precisely the same way. The lifts of the orbits to period three are summarized in Table 1.

6.2. Non-periodic Orbits

Every chaotic orbit in the image lifts to $g-1$ chaotic orbits in the cover. The symbolic name of each lift is determined as follows. Associate the matrix $T_{\rm str}$ or $T_{\rm cyc}$ to each symbol of the image orbit: for example $01101\ldots \to T_{\rm str}T_{\rm cyc}T_{\rm cyc}T_{\rm str}T_{\rm cyc}\ldots$. An initial condition in the cover is represented by an array, for example an initial condition in the branch line 2 in the cover is identified by the array $A_2 = (0, 1, 0, 0)$. After one topological period the initial condition has moved to branch line j, defined by $(A_2)_i(T_{\rm str})_{ij} = 1$. The location after the next topological period is determined similarly — by multiplying the array on the right by $T_{\rm cyc}$. This encoding proceeds as far as desired. In this way chaotic symbol sequences with arbitrary length can easily be encoded. By changing the complexity of the cover we can obtain sequences containing as many different symbols as desired. It is clear that each lift has a distinct trajectory. For the chaotic trajectory starting 01101... and initial condition on branch line 2, the itinerary in the cover is (2)41241.... Initial conditions on other branch lines generate other encodings of the non-periodic string 01101... .

7. Index of Covering Orbits

An orbit in the image attractor is assigned an index that depends both on the orbit and the cover to which it is lifted. The index has three interpretations.

Table 2. The orbits described in Table 1 circle each of the g holes in the bounding torus an integer number of times. For each orbit the set of integers provides its rotation index. Rotation indices do not uniquely identify orbits.

Period	Image	Cover	A	B	C	a	b
1	0	1	1	0	0	0	0
		24	0	1	0	0	0
		3	0	0	1	0	0
1	1	1234	1	1	1	1	1
2	01	11 24	2	1	0	1	0
		23 34	0	1	2	0	1
3	001	112 423 334 241	3	3	3	1	1
3	011	112 334	2	1	2	1	1
		124	1	1	0	1	0
		234	0	1	1	0	1

Group theoretic: The permutation matrix for the orbit is a product of the matrices T_{str} and T_{cyc} in a particular order determined by the symbolic dynamics of the image orbit. The two matrices T_{str} and T_{cyc} generate a subgroup of S_{g-1}.

Dynamical: The permutation matrix that is assigned to each orbit in the image describes the allowed transitions in the lifts of that orbit into the cover. This summarizes the dynamics, at least for the orbit under study. The cyclic structure of the permutation matrix determines the periods of the covering orbits. Some examples are presented in Table 1.

Topological: The periodic orbits that cover the image orbit rotate around the holes in the bounding tori. The rotation index is a topological index that can be computed for each lifted orbit. Some examples are presented in Table 2.

We give examples of the topological rotation index for lifts of the periodic orbits 0, 1, 01, 001, and 011 from the image Smale horseshoe branched manifold to the covering orbits in the genus-5 bounding torus in Table 2. This table identifies the lifts of the orbits and shows how often each of these lifts rotates around each of the three singularity free holes (A, B, C) and the two singular holes (a, b). This 5-tuplet is a topological index, the rotation index, for each of the lifted orbits.

The components of the rotation index for the periodic orbits given in Table 2 can be read directly from the symbol name of the orbits. The number of times an orbit encircles a singularity free hole (e.g., B) is the number of times a particular symbol (either 2 or 4) appears in the orbit name. The symbol describes any one of the branch lines attached to that hole. The number of times an orbit encircles a hole with singularities (e.g., b) is the number of times a particular symbol *pair* (either 23 or 34) appears in the orbit name. This pair describes either of the two ways the flow passes the hole with singularities.

The integers in this table are in fact a homotopy index. Any single lift can circle any of the holes (A, B, C) an integer number of (or zero) times. However, the set of all the lifts of an image orbit of period p must circle each of the holes (A, B, C) a total of p times. This comes about because each of these holes is the lift of the hole in the middle of the horseshoe branched manifold (the torus that contains it). An image orbit of period p circles this hole p times in the image. In the cover, each lift of the single hole in the image (holes A, B, etc) is circled p times by the set of lifts. That is, $\sum n_A(orb) = p$, where the sum extends over all the orbits that cover the image orbit. The same holds true for the sums of the indices of all singularity-free holes: $\sum n_B(orb) = \sum n_C(orb) = p$. This result is general for lifts to branched manifolds enclosed in any bounding torus. The corresponding relation for the holes with singularities is $\sum n_a(orb) = \sum n_b(orb) = p_1$, where the symbolic representation of the image orbit has p_0 symbols 0 and p_1 symbols 1. More generally (cf. Sec. 9) p_1 is the number of times the matrix $T_{\rm cyc}$ appears in the product for the index. The invariant indices can be verified by inspection of Table 2. These results generalize for lifts into arbitrary bounding tori.

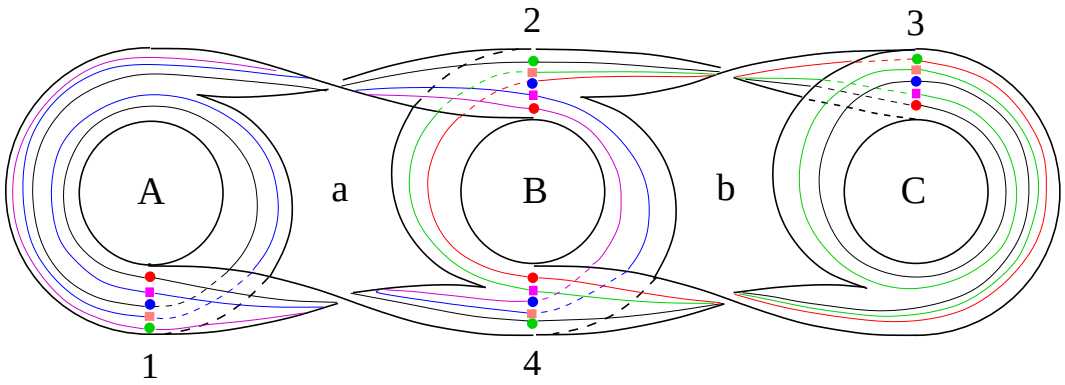

Figure 9. The lifts of the horseshoe orbits 01 and 011. If the intersections with the branch line(s) are labeled $(i) \to (v)$ from inside to outside, the period two orbit 01 visits $(ii) \to (iv) \to (ii)$ etc., and the period-three orbit 011 visits $(i) \to (iii) \to (v)$.

8. Links of Lifts

The topological organization of the periodic orbits on a knot holder is specified in terms of their linking numbers. For example we consider the pair of orbits with symbolic names 01 and 011 on the image branched manifold (the Smale horseshoe). Their linking number can be computed algorithmically once their symbolic name and the structure of the branched manifold are known. The period two orbit 01 exhibits one positive crossing with itself, the period three orbit 011 exhibits two, and the two orbits 01 and 011 exhibit four ([3], figure 5.18, p. 197). This information is summarized as

	01	011
01	+1	+4
011	+2	+2

Table 3. Signed crossing information for lifts of horseshoe orbits 01 and 011 into the branched manifold of figure 5. The lifts are shown in figure 9. On and above diagonal: number of crossings of the lifted orbits, including signs. On diagonal: self-linking number of lifted orbits and below diagonal linking number (half the sum of signed crossings) of lifted orbits.

		01		011		
		1124	2334	112334	124	234
01	1124	+1	+2	+4	+2	+2
	2334	+1	−1	+1 − 3	+2	+1 − 1
	112334	+2	−1	+1 − 1	+2	+1 − 1
011	124	+1	+1	+1	0	+2
	234	+1	0	0	+1	0

This crossing information is exhibited on and above the major diagonal. There is a total of $1 + 2 + 4 = 7$ crossings. The self-linking number of an orbit with itself is the signed number or crossings of that orbit with itself, and the linking number of two different orbits (a topological invariant) is half their signed number of crossings. The self-linking numbers and linking numbers are exhibited on and below the major diagonal of the matrix above. We obtain directly from this matrix $SL(01) = +1$, $SL(011) = +2$, $L(01, 011) = \frac{1}{2}(+4) = +2$.

When the orbits are lifted to a covering branched manifold, each orbit can lift to a set of orbits. The covering orbits do not necessarily have the same topological period. For example, the period-three orbit 011 lifts to orbits 124, 234, and 112334 (figure 8) in the cover. A linking number can be computed for each pair of lifted orbits. In the covering branched manifold the total number of crossings is $4 \times (1 + 2 + 4) = 28$. Of these 28 crossings, all seven approaching branch line 3 are negative, while all crossings of orbit segments entering the other three branch lines are positive. As a result the total number of signed crossings in all covering orbits is $+21 - 7 = +14$. Thus, the sum over all covering orbits of the self-linking numbers + twice the sum of the linking numbers of all orbit pairs is +14. The signed crossing information of the covering orbits is summarized in Table 3.

Inspection of the table reveals that the invariants of the lifts are preserved. For example, there are $4 = 4 \times 1$ crossings of lifts of the period-two orbit with lifts of the period-two orbit, three positive, one negative. For lifts of the period-three orbit with lifts of the period-three orbit, there are $8 = 4 \times 2$ crossings, two negative. And for lifts of the period-two orbit with lifts of the period-three orbit, there are $16 = 4 \times 4$ crossings, one quarter of which are negative.

The table of linking numbers of orbit pairs depends on the symbol name of the image orbits and the branched manifold into which they are lifted. On the other hand, the rotation index depends only on the symbol name of the image orbits and the bounding

torus into which these orbits are lifted (and not the particular branched manifold to which they are lifted).

9. Generic Covers

The covers of the horseshoe described above have not been generic. This is because the "tear point" for the covers has been located at the maximum in the return map of the image [12]. This is indicated in figure 10(a). In this figure T_1 indicates where the tear point has been located for the class of covers considered in Sec. V. More generally ("generically"), the tear point can be taken anywhere along the branch line of the image, for example at the point T_2 shown in figure 10(a). When this is the case, the lifts of the squeeze-and-stretch unit into the cover have the form shown in figure 10(b). When the tear point T_2 occurs between the points β and γ where the period-three orbit 011 meets the branch line in the image, the segments of covering orbits over the flow with point $\beta = 110$ as initial condition proceeds through flow tube determined by the part $T_{\rm str}$ of the transition matrix. In this case the index for the period-three orbit is determined from the identification

$$011 \rightarrow T_{\rm str}T_{\rm str}T_{\rm cyc} \simeq (1234)$$

Similar results hold for lifts of all orbits from the image attractor to covering attractors.

10. Conclusions

It has been remarked that the studies of Lie group theory, singularity theory, and dynamical systems theory have many similarities. As a result many useful analogies among these three branches of mathematics ought to exist [3].

One intriguing possibility is that Cartan's covering theorem for Lie algebra - Lie groups ought to have a parallel for dynamical systems. Determining this analogy should be especially useful, now that systematic image and covering relations have been developed for strange attractors.

In this work we have described this analogy. In Lie group theory there is a universal covering group, defined for each Lie algebra. All Lie groups with the same Lie algebra are topologically distinct: they are identified by their homotopy group, related to a particular discrete invariant subgroup of order $|D|$. The universal covering group is simply connected. The maximal discrete invariant subgroup maps the universal covering group down to a "least simply connected" $|D| \rightarrow 1$ image Lie group. In this group the neighborhood of the identity is covered by $|D|$ group operations, each of which is topologically like the identity except in its multiplication properties.

The situation for low dimensional dynamical systems ($d_L < 3$) is similar. There is some smallest, least multiply connected image dynamical system. We have chosen this to describe the mechanism most commonly encountered in physical systems so far. This is the Smale horseshoe mechanism, described by a simple branched manifold with

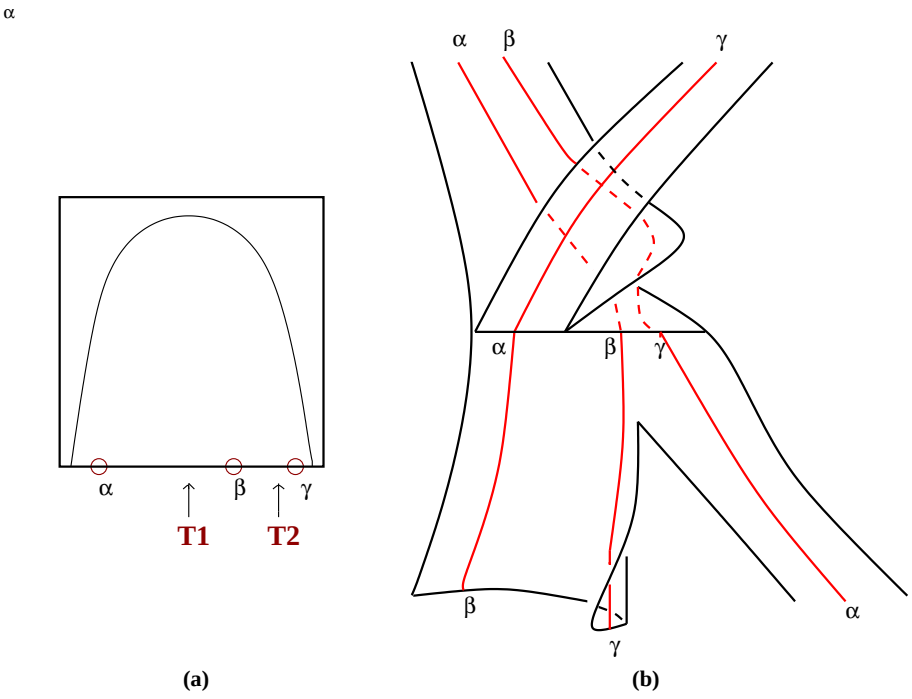

Figure 10. (a) Return map on the branch line of the horseshoe branched manifold. The period-three orbit 011 intersects the branch line successively at α, β, γ. The tear point for the lift shown in figure 5 occurs at the location of the maximum T_1, which is non-generic. A generic tear point at T_2 produces a different set of covering orbits. (b) Structure of the squeeze-stretch units for the generic tear point T_2. The orbit segments transit flow tubes with labels 0, 0, and 1. The transition matrix for this lift is $011 \rightarrow T_{\rm str}T_{\rm str}T_{\rm cyc}$.

two branches. The branch line, together with the two inflow branches that describe squeezing, and the two outflow branches that describe stretching, are analogous to the neighborhood of the identity in the "least simply connected" Lie group, with the branch line playing the role of the identity group operation. It has many covers.

A $1 \rightarrow (g-1)$ local diffeomorphism lifts the image into a bounding torus with genus g. The branched manifold enclosed by this torus has $g-1$ branch lines. Each branch line is analogous to a point in the universal covering group that maps into the identity of the "least simply connected" image Lie group. The flow tubes (inflows and outflows) connected to each branch line are analogous to the neighborhoods of operations in the universal covering group that are lifts of the identity in the "least simply connected" image Lie group.

As for Lie groups, so for strange attractors. In the image the outflow from the branch line flows back, in one topological period, to the branch line. In the image group, the product of two operations in the neighborhood of the identity remains in the neighborhood of the identity. In the covers this is no longer true. Part of the outflow from one branch line in connected covers always flows to another branch line. In the universal covering group, the product of two group operations, each in the neighborhood

of a point that maps to the identity, typically lies in a different neighborhood.

All the covers of the horseshoe have been classified. The lifts are distinguished first by a bounding torus of genus g ($g \geq 3$). These tori are characterized by a transition matrix $T = T_{\rm str} + T_{\rm cyc}$ (equation (1)) that is the sum of two permutation matrices in S_{g-1}. The bounding tori are labeled by words of period $g-1$ (e.g., $ABCB$, $abba$). The number of canonical forms of genus g grows exponentially with g with an entropy of log(3) [15]. Once a canonical form has been chosen, all covering branched manifolds compatible with that canonical form can be introduced. They consist of $g-1$ squeeze-and-stretch units of the type shown in figure 3(a). The covering branched manifolds are differentiated by the helicity of the transition branches, or flow tubes. This is shown by "dressing" the transition matrix, $T = T_{\rm str} + T_{\rm cyc} \rightarrow Tor$, as indicate in equation (2). Different Torsion matrices describe different branched manifolds. Periodic and chaotic orbits in the image attractor can be lifted into periodic and chaotic orbits in the covering dynamical system. This is most simply done by assigning an index to the image orbit, as in equation (3). For a periodic orbit the index is a permutation group operation ("set of cycles"). It has a group theoretic interpretation, a dynamical interpretation, and a topological interpretation. The index of an orbit can be used to determine the symbolic names of all the lifts of that orbit. Each lift possesses a rotation index that depends on the bounding torus but is independent of the enclosed branched manifold. On the other hand, the topological organization of the lifted orbits (their linking numbers) depends on the particular branched manifold that is chosen within the bounding torus. The methods introduced here and illustrated for the particular case used as a vehicle for our discussion ($p = 2, 3; n = 4; g = 5$) are valid for lifts:

(1) of any periodic orbit characterized by a symbol string 01... of length p or any chaotic trajectory in the image [c.f., equation (3)];

(2) into any branched manifold characterized by a torsion matrix Tor [c.f., equation (2)];

(3) enclosed by any bounding torus of genus $g \geq 3$ characterized by a transition matrix $T = T_{\rm str} + T_{\rm cyc}$ [c.f., equation (1)].

References

[1] Gilmore R 1974 *Lie Groups, Lie Algebras, and Some of Their Applications*(New York: Wiley)

[2] Gilmore R 1981*Catastrophe Theory for Scientists and Engineers*(New York: Wiley)

[3] Gilmore R and Lefranc M 2002 *The Topology of Chaos* (New York:Wiley)

[4] Birman J and Williams R F 1983 Knotted periodic orbits in dynamical systems I: Lorenz's equations *Topology* **22** 47-82

[5] Birman J and Williams R F 1983 Knotted periodic orbits in dynamical systems II: Knot holders for fibered knots *Contemporary Mathematics* **20** 1-60

[6] Gilmore R 1998 Topological analysis of chaotic dynamical systems Revs. Mod. Phys. **70**(4) 1455

[7] Miranda R and Stone E 1993 The proto-Lorenz system *Phys. Lett. A* **178** 105-113

[8] Letellier C and Gilmore R 2001 Covering dynamical systems : Two-fold covers *Physical Review* E **63** 16206

[9] Gilmore R and Letellier C 2003 Dressed Symbolic Dynamics *Phys. Rev.* E **67** 036205

[10] Tsankov T D and Gilmore R 2003 Strange attractors are classified by bounding tori *Physical Review Letters* **91**(13) 134104
[11] Tsankov T D and Gilmore R 2004 Topological Aspects of the Structure of Chaotic Attractors in R^3 *Phys. Rev.* E **69** 056206 1-11
[12] Byrne G, Gilmore R. and Letellier C 2004 Distinguishing between folding and tearing mechanisms in strange attractors *Phys. Rev.* E **70** 056214
[13] Peixoto 1961 Structural Stability on two-dimensional manifolds *Topology* **2** 101-121
[14] Lorenz E N 1963 Deterministic non periodic flow *Journal of the Atmospheric Sciences* **20** 130-141
[15] Katriel J and Gilmore R Entropy of bounding tori (unpublished)